Manuscript Details

Manuscript number	JMBBM_2019_1264_R2
Title	The Use of µCT and Fractal Dimension for Fracture Prediction in Osteoporotic Individuals
Article type	Research Paper

Abstract

Osteoporosis (OP) is a widespread condition with commonly associated fracture sites at the hip, vertebra and wrist. This study examines the effects of age and osteoporosis on bone quality by comparing the efficacy of using parameters which indicate bone quality (both traditional clinical parameters such as bone mineral density (BMD), as well as apparent Young's modulus determined by finite element analysis, among others) to predict fracture. Non-fracture samples were collected from the femoral heads of 83 donors (44 males, 39 females), and fracture samples were obtained from the femoral heads of 17 donors (female). Microarchitectural parameters (Bone Volume/Total Volume [BV/TV], Bone Surface/Bone Volume [BS/BV], Tissue Mineral Density [TMD, etc.]) were measured from µCT of each sample as well as 2D and 3D fractal dimension (D2D and D3D respectively). A cube was cropped from µCT images and an isotropic hexahedral element was assigned to each voxel. Finite element analysis was used to calculate the Young's modulus for each sample. Overall, values for microarchitectural characteristics, fractal dimension measurements and Young's Modulus were consistent with values within literature. Significant correlations are observed between age and BV/TV for non-fracture males and females, as well as between age and volumetric BMD (vBMD) for the same groups. Significant differences are present between age-matched non-fracture and fracture females for BV/TV, BS/BV, vBMD, TMD, D2D, D3D, (p < 0.01 for all). Properties which are not age dependent are significantly different between age-matched non-fracture and fracture specimens, indicating OP is a disease, and not just an accelerated aging process.

Keywords	Bone µCT; Osteoporosis; Femoral Head; Finite Element Analysis; Fractal Dimension
Taxonomy	Materials Property, Fracture, Biomedical Materials
Manuscript category	Hard Tissues
Corresponding Author	Emily Arnold
Corresponding Author's Institution	NESLI Cranfield University
Order of Authors	Emily Arnold, John Clement, Keith Rogers, Fabio Garcia-Castro, Charlene Greenwood
Suggested reviewers	Rita Hardiman, Nick Stone, Christopher Hall

Submission Files Included in this PDF

File Name [File Type]

JMBBM Cover Letter.pdf [Cover Letter]

Reviewer Comment Reply.pdf [Response to Reviewers]

JMBBM Submission.pdf [Manuscript File]

declaration-of-competing-interests.pdf [Conflict of Interest]

Author Statement.pdf [Author Statement]

To view all the submission files, including those not included in the PDF, click on the manuscript title on your EVISE Homepage, then click 'Download zip file'.

Research Data Related to this Submission

There are no linked research data sets for this submission. The following reason is given:
Data will be made available on request

1   **The Use of µCT and Fractal Dimension for Fracture Prediction in Osteoporotic**

2   **Individuals**

3

4   Emily L Arnold, BSc, MSc (corresponding author)

5   Cranfield Forensic Institute, Cranfield University, Shrivenham, UK

6   +44 (0) 1793785257   e.arnold@cranfield.ac.uk

7

8   John Clement, BDS, LDS RSC, PhD

9   Melbourne Dental School, University of Melbourne, Australia

10

11   Keith D Rogers, BSc, PhD

12   Cranfield Forensic Institute, Cranfield University, Shrivenham, UK

13   Engineering & Physical Science grants EP/R024316/1 and EP/K020196/1

14

15   Fabio Garcia-Castro

16   QUIBIM S.L., Valencia, ES

17

18   Charlene Greenwood, BSc, MSc, PhD

19   School of Chemical and Physical Sciences, University of Keele, UK

20   Engineering & Physical Science grants EP/R024316/1 and EP/K020196/1

21

22

25

1   **Abstract**

2   Osteoporosis (OP) is a widespread condition with commonly associated fracture sites at the

3   hip, vertebra and wrist. This study examines the effects of age and osteoporosis on bone quality

4   by comparing the efficacy of using parameters which indicate bone quality (both traditional

5   clinical parameters such as bone mineral density (BMD), as well as apparent Young's modulus

6   determined by finite element analysis, among others) to predict fracture. Non-fracture samples

7   were collected from the femoral heads of 83 donors (44 males, 39 females), and fracture

8   samples were obtained from the femoral heads of 17 donors (female). Microarchitectural

9   parameters (Bone Volume/Total Volume [BV/TV], Bone Surface/Bone Volume [BS/BV],

10   Tissue Mineral Density [TMD, etc.]) were measured from µCT of each sample as well as 2D

11   and 3D fractal dimension (D^{2D} and D^{3D} respectively). A cube was cropped from µCT images

12   and an isotropic hexahedral element was assigned to each voxel. Finite element analysis was

13   used to calculate the Young's modulus for each sample. Overall, values for microarchitectural

14   characteristics, fractal dimension measurements and Young's Modulus were consistent with

15   values within literature. Significant correlations are observed between age and BV/TV for non-

16   fracture males and females, as well as between age and volumetric BMD ($_v$BMD) for the same

17   groups. Significant differences are present between age-matched non-fracture and fracture

18   females for BV/TV, BS/BV, $_v$BMD, TMD, D^{2D}, D^{3D}, ($p < 0.01$ for all). Properties which are

19   not age dependent are significantly different between age-matched non-fracture and fracture

20   specimens, indicating OP is a disease, and not just an accelerated aging process.

OP Osteoporosis; BMD bone mineral density; BV/TV bone volume/total volume; BS/BV bone surface/bone volume; TMD tissue mineral density; D^{2D} 2D fractal dimension; D^{3D} 3D fractal dimension; $_v$BMD volumetric bone mineral density.

1 Introduction

Osteoporosis (OP) is a widespread condition affecting over 3 million individuals in the UK (1 in 3 women and 1 in 5 men (International Osteoporosis Foundation, 2015)), with more than 500,000 fragility fractures sustained each year (NHS, 2016). Fracture sites that are most commonly associated with OP include the hip, vertebra and wrist. Although hip fractures are slightly less prevalent than wrist fractures they have significant repercussions as they are associated with the highest mortality rate post-fracture and a severe reduction in an individual's independence (International Osteoporosis Foundation, 2015).

OP is characterised by the reduction in bone mass and decline of trabecular microarchitecture as the condition progresses (Osterhoff et al., 2016); typically, a reduction in the trabecular mass, either by the loss of trabeculae or a decrease in average trabecular thickness is observed. This reduction in bone mass is often associated with a decrease in bone strength. Bone strength is often attributed to a combination of bone density and 'bone quality,' where bone quality is considered macroarchitecture, microarchitecture and physicochemical properties (Teo et al., 2006; Yerramshetty and Akkus, 2013). Several techniques are currently employed to evaluate fracture risk, the most prominent being dual-energy X-ray absorptiometry (DXA).

Bone mineral density (BMD) is widely used as a predictor of fracture risk. DXA (which measures areal BMD ($_a$BMD)) is currently the gold standard used to diagnose OP by comparing a patients $_a$BMD to a healthy young database (with a T-score) or to a healthy age- and sex-matched database (with a Z-score) (Kanis et al., 2013). $_a$BMD is shown to account for 40% - 60% of trabecular strength, depending on the site examined (Engelke et al., 2016; Jiang et al.,

---

OP Osteoporosis; DXA dual-energy X-ray absorptiometry; BMD bone mineral density; $_a$BMD areal BMD; $_v$BMD volumetric BMD; HR-pQCT high resolution peripheral quantitative CT; FD fractal dimension; MRI magnetic resonance imaging; FEA finite element analysis; TbTh trabecular thickness; TbSp trabecular spacing; BS bone surface; BV bone volume; TV total volume; TMD tissue mineral density; D^{2D} 2D fractal dimension; D^{3D} 3D fractal dimension; MIL mean intercept length; E_z apparent Young's modulus in z direction.

1   1999), although bone strength, even as measured by a proxy such as $_a$BMD, is not the only

2   determinant of fracture risk. Additional tools, such as the FRAX® tool, are currently widely

3   used and augment $_a$BMD with an individual's features such as previous fractures, age, height

4   and weight (Kanis et al., 2013). The diagnosis with the greatest efficacy will be one that can

5   predict early onset OP with a greater sensitivity and specificity than DXA. The most effective

6   way to accomplish this is to increase the number of parameters by which bone quality is

7   measured, particularly trabecular quality. Several techniques are currently available which may

8   provide deeper insight into OP, and aid in early diagnosis.

9   The first of these techniques is high resolution peripheral quantitative CT (HR-pQCT) which

10 has the ability to reliably measure trabecular structure *in vivo*. The increase in use of HR-pQCT

11 brought studies involving the use of microarchitectural properties to diagnose OP,

12 demonstrating increased effectiveness (van Reitbergen and Ito, 2015). Significant correlations

13 are seen between microarchitectural parameters (such as trabecular thickness and trabecular

14 spacing) and fracture status (Greenwood et al., 2018).

15 Additionally, a parameter which has been used in histomorphometry applied to radiographs is

16 the fractal dimension (FD), employed to characterise the complexity of the trabecular structure

17 (Benhamou et al., 2001; Cortet et al., 2004; Fazzalari and Parkinson, 1996; Jiang et al., 1999).

18 Most recently this parameter has been derived *in vivo* from higher-resolution non-invasive

19 imaging techniques (such as HR-pQCT and magnetic resonance imaging (MRI)) to study OP

20 individuals and *ex vivo* from μCT. In previous OP induced longitudinal rat model studies, FD

21 was shown to be the parameter that can distinguish the reduction in trabecular structure earliest,

22 which is a characteristic of OP (Audran et al., 2001). Studies that incorporate FD are currently

23 limited by the sample size (for example, N = 12 for healthy samples and N = 12 for osteoporotic

24 samples (Alberich-Bayarri et al., 2010)) or use of animal models (Audran et al., 2001).

1   Finite element analysis (FEA) has been used to increase accuracy of fracture prediction, with

2   varying degrees of success (van Rietbergen and Ito, 2015). Several approaches are employed,

3   depending on imaging technique (e.g. DXA, MRI, CT) and the resolution of the images taken

4   (>200 µm for clinical CT, 40-120 µm for HR-pQCT, and ~16 µm for µCT) (Burghardt et al.,

5   2011). The analysis power of FEA (particularly µ-FEA, in this context meaning FEA which is

6   applied to bone microstructure (van Rietbergen and Ito, 2015)) has grown dramatically in the

7   past 20 years (Keaveny et al., 2010; Kopperdahl et al., 2014; MacNeil and Boyd, 2008;

8   Alberich-Bayarri et al., 2008; Naylor et al., 2013; Osterhoff et al., 2016). Using this increase

9   in capability, studies have shown that FEA can more accurately predict mechanical properties

10   (such as fracture load and Young's modulus) than models which take into account either $_a$BMD

11   or microarchitectural parameters (Cody et al., 1999; van Rietbergen and Ito 2015). The µ-FEA

12   and FEA in general is becoming more feasible, the relatively high resources necessary for this

13   analysis still acts as a barrier here. Mechanical properties of bone, often Young's modulus, are

14   used to assess fracture risk (Engelke et al., 2016), obtained both experimentally and with µ-

15   FEA. Most studies which validate µ-FEA values for Young's modulus against experimental

16   values have relatively small numbers (N = 6 (Chevalier et al., 2007)). This is also an issue in

17   studies which compare Young's modulus with various microarchitectural parameters (N = 23

18   for femoral neck samples (Morgan and Keaveny, 2001)).

19   This study examines the effects of age and osteoporosis on bone quality by comparing the

20   efficacy of using parameters which indicate bone quality (both traditional clinical parameters

21   such as BMD, as well as apparent Young's modulus determined by FEA, among others) to

22   predict fracture. The aim of this study is to determine parameters where the largest differences

23   are observed through comparison of fracture and non-fracture samples. Correlations of

24   microarchitectural and micromechanical parameters with age will provide insight into

25   trabecular changes due to aging. Similarly, correlations between microarchitectural and

micromechanical parameters will examine which of these parameters provide the best estimation of the mechanical properties of bone (predicted here using µ-FEA). Determination of parameters where the most discriminatory power is found has the potential to improve the efficacy of fracture prediction.

A study on age and microarchitectural properties of the samples used here has been previously published (Greenwood, 2018). Several other similar studies have been published before, however, this study will provide the most comprehensive analysis of microarchitectural characteristics and mechanical properties for a sample of non-fracture and fracture femoral heads from a human population.

2 Materials and Methods

2.1 Bone Specimens

Bone specimens used within this study have been previously described in detail (Greenwood, 2018). As DXA measurements were not available for any samples, this study focuses on groups of fracture and non-fracture specimens rather than osteoporotic and non-osteoporotic specimens. A sample set of femoral heads were collected from the Melbourne Femur Collection from 83 donors (44 males, 39 females) who had never suffered a femoral fracture and had either died of natural causes or due to a sudden fatal accident. The specimens were collected with next-of-kin informed consent. The femoral heads were selected at random, across a wide range of 20 – 93 years of age. Ethical approval for the collection and use of these specimens was provided by The University of Melbourne. All individuals were Anglo-Celtic and followed modern, urbanised lifestyles.

The fracture population used here was a sub-set of the female fracture sample previously published (Greenwood, 2018). A sample set of femoral heads were collected from 17 donors

1 (female) who were diagnosed as osteoporotic and had suffered fragility fractures at the femoral

2 neck consequently requiring hip replacement surgery. Age of donors ranged from 73 to 91

3 years old. Ethical approval for the collection and use of these specimens was provided by

4 Gloucestershire NHS trust REC.

5 A summary of average values for microarchitectural parameters for the entire sample (both

6 fractured and non-fractured) used by Greenwood et al (2018) can be found in Table 1. BV/TV,

7 BS/BV, TbTh, TbSp, vBMD, and TMD were analysed within the stated previous study; FD

8 and FEA results are analysed specifically within this study.

9 *Table 1: Average values (± SEM) for the microarchitectural parameters for fracture and non-*

10 *fracture groups for the sample used by Greenwood et al (2018).*

	Non-Fracture		Fracture	
	Female	Male	Female	Male
Donors	39	39	30	7
Number of Specimens	39	39	58	23
Age Range (yrs)	20-90	21-93	59-91	74-84
Age Mean (yrs)	66.18 ± 17.92	64.75 ± 19.00	82.47 ± 6.43	76.90 ± 2.72
BV/TV	0.30 ± 0.01	0.32 ± 0.01	0.18 ± 0.01	0.18 ± 0.01
BS/BV (mm^{-1})	110.83 ± 0.24	10.10 ± 0.22	16.06 ± 0.40	17.84 ± 0.53
TbTh (mm)	0.19 ± 0.004	0.20 ± 0.005	0.13 ± 0.004	0.11 ± 0.003
TbSp (mm)	0.44 ± 0.01	0.45 ± 0.01	0.60 ± 0.02	0.52 ± 0.02
$_v$BMD (g cm^{-3})	0.50 ± 0.02	0.52 ± 0.02	0.30 ± 0.01	0.31 ± 0.02
TMD (g cm^{-3})	1.64 ± 0.01	1.62 ± 0.01	1.61 ± 0.01	1.65 ± 0.01

11

12 Population characteristics for all donors are provided in Table 2. Due to the lack of male

13 fracture specimens, comparisons were made between non-fracture males and females, and

14 between non-fracture females and fracture females.

15 *Table 2: Population characteristics for donors (± SEM), differentiated according to sex and*

16 *fracture status.*

				Age Matched (73+ years)	
	Non-Fracture		Fracture	Non-Fracture	Fracture
	Male	Female	Female	Female	Female

Donors	44	39	17	18	17
Age Range (yrs)	21-93	20-90	73-91	73-90	73-91
Age Mean (yrs)	64.75 ± 19.00	65.71 ± 17.92	83.18 ± 5.08	80.50 ± 5.06	83.18 ± 5.08

1

2 *2.2 Sample Preparation*

3 The procedure for sample preparation has been described in detail previously (Greenwood,

4 2018). Core specimens were obtained by a combination of trephine coring and mechanical

5 cutting. Specimens were randomly sampled to minimise orientation bias. Prior to imaging, the

6 cores were cleaned carefully using a warm water jet to remove bone marrow from within the

7 trabecular spaces. For further information regarding the sample preparation refer to

8 Greenwood, et al (2018). Image analysis for analysis of FD and subsequent FE analysis was

9 performed using the Bone Microarchitecture tool in Quibim Precision® v2.3 (Quibim S.L,

10 Valencia, Spain).

11

12 *2.3 Micro Computed Tomography (μCT)*

13 Bone microarchitecture was examined with micro computed tomography (μ-CT). Each

14 specimen was scanned using a Nikon CT H225 (X-Tek Systems Ltd, Tring, Hertfordshire, UK)

15 cone beam μ-CT scanner operated at 35 kV, and 115 μA. The geometric magnification

16 produced a voxel dimension of 15-25 μm. Voxel size was inconsistent due to the natural

17 variation within the size of human femoral heads. Noise reduction and beam hardening

18 corrections were applied to the data and VG Studio Max 2.2 (Volume Graphics GmbH,

19 Heidelberg, Germany) utilised to visualise and quantify several microarchitectural features.

20 These included trabecular thickness (TbTh) and spacing (TbSp), surface area (BS), material

21 volume (BV) and total volume (TV). VG Studio Max relies on the plate assumption to calculate

22 trabecular parameters. Consequently, while TbTh and TbSp are reported for completeness, they

are excluded from any further analysis as they are not independent. QRM Micro CT-HA (QRM GmbH, 91096 Möhrendorf, Germany) calibration phantoms, which differ in known tissue mineral density (TMD) values, were scanned and reconstructed under the same conditions as the specimens. The mean grey scale values taken from the attenuation histograms for these phantoms were then used to construct a calibration curve of TMD values and grey scales. This allowed calculation of tissue mineral density values for the trabecular specimens. TMD values were then used to determine bone mineral density values ($_v$BMD) according to

$$_v\text{BMD} = \text{TMD} \times \text{BV/TV}. \qquad (1)$$

TMD refers to the density measurement restricted to within the volume of calcified bone tissue, and excludes any surrounding soft tissue, whereas $_v$BMD is the combined density in a well-defined volume.

2.4 Fractal Dimension Analysis

Two-dimensional and three-dimensional Minkowski fractal dimensions (D^{2D} and D^{3D} respectively) were calculated using a box counting algorithm (validated using the Sierpinski Triangle where $D^{2D} = 1.585$) and Equation 2:

$$\ln N = -D \ln \lambda + k \qquad (2)$$

where N is the number of contour boxes, λ is the box size, D is the fractal dimension parameter (either D^{2D} or D^{3D}), and k is a proportionality constant (Alberich-Bayarri et al., 2010). The fractal dimension measures the surface complexity of an object and relies on the principle that what is being measured is self-similar at differing scales. Within the context of trabecular bone, FD is known to correlate with both BV/TV, and BS/BV (Alberich-Bayarri et al., 2010; Fazzalari and Parkinson, 1996).

2.5 Finite Element (FE) Analysis

Processing of data and FEA was carried out as described by Alberich-Bayarri et al (2008). The principle structural direction was selected by using the mean intercept length (MIL) to determine the main trabeculae direction, which was selected as the new z-axis. The largest possible cube was cropped from the rotated sample along the new axes. Inhomogeneities were corrected within the image (an inhomogeneity correction filter was applied to images to correct for potential signal intensity heterogeneities), for more detail see Alberich-Bayarri et al (2008). Each image was then binarized using Otsu's algorithm. Each voxel was converted directly into isotropic hexahedral (brick) elements. Elements were set to have properties of compact bone (Young's Modulus, E = 10 GPa; Poisson's ratio, σ = 0.3) (Alberich-Bayarri et al., 2008; Fung, 1993; Newitt et al., 2002).

Apparent modulus was calculated along the z-axis (E_z). The solution of the FEA linear system of equations was solved using Ansys (Version 13.0) for a homogenised isotropic structure. Homogenised isotropic structure is used in this context to mean the elastic modulus for each voxel was consistent and all voxels were isotropic in nature. The apparent elastic modulus for the z-axis was obtained using Equation 3:

$$E_z = \frac{1}{\varepsilon A} \sum_n F_n \tag{3}$$

where ε is strain, A is the surface area over which a force is applied, and F is the force applied.

2.6 Statistical Analysis

Linear regression analysis was carried out to statistically assess correlations between microarchitecture parameters and age for the non-fracture group. Linear regression analysis was also carried out on microarchitecture parameters and E_z for both the non-fracture and fracture groups to evaluate the relationship between microarchitecture and apparent Young's

modulus. Anderson–Darling tests were carried out to determine whether data are normally distributed. Student's T-tests (for normally distributed data) and Mann-Whitney U tests (for non-normally distributed data) were performed on age-matched female non-fracture and fracture samples to determine statistically significant differences. Diagnostic tests to determine both sensitivity and specificity of several microarchitectural parameters, fractal dimensions and E_z were performed to determine the relative weight parameters should be given. For all parameters, the midpoint between the mean of the age-matched non-fracture female sample and the fracture female sample was used as the cut-off point.

3 Results

A summary of the major quantitative values for the parameters measured (e.g. microarchitectural quality, fractal dimension and mechanical properties) of trabecular bone from human fracture and non-fracture specimens are reported in Table 3 (mean and standard error of the mean), with parameters further correlated to age (Table 4). Microarchitectural parameters were correlated to apparent Young's modulus in the direction of principle loading (E_z) as determined through FEA. Results of the statistical testing applied to each characteristic parameter are summarised within Table 3.

Table 3: Average values (in bold) and the associated errors ($\pm$ SEM) for properties of fracture and non-fracture groups. Non-normal datasets denoted by *. p-Values for age matched Student's T-tests of female fracture (n = 18) and female non-fracture (n = 17) groups (Mann-Whitney U tests for pairs including non-normal data sets), for each parameter are also provided. Values taken from literature for human samples where the femoral heads were sampled. Sample numbers for referenced studies are denoted as follows: [†] N = 50 (Perilli et al., 2008); [‡] N = 10 (Li et al., 2012); [§] N = 9 (Zhang et al 2010); [II] N = 77 (Wu et al., 2015); [¶] N = 14 (Morgan and Keaveny, 2001).

| | Non-Fracture | | Age Matched | | | Literature | |
	Males	Females	Non-Fracture Females	Fracture Females	p-Value Females	Non-Fracture	Fracture

N	44*	39*	18	17	--	--	--
BV/TV	**0.32** ± 0.01	**0.30** ± 0.01	**0.28** ± 0.01*	**0.18** ± 0.01	<0.001*	**0.27** ± 0.01[†]	**0.19** ± 0.01[‡]
BS/BV (mm^{-1})	**10.10** ± 0.22	**10.83** ± 0.24	**11.17** ± 0.28	**16.16** ± 0.58	<0.001	--	**14.51** ± 0.75[§]
TbTh (mm)	**0.20** ± 0.01	**0.19** ± 0.01	**0.18** ± 0.01	**0.13** ± 0.01	>0.05	**0.13** ± 0.01[†]	**0.17** ± 0.01[‡]
TbSp (mm)	**0.45** ± 0.01	**0.44** ± 0.01	**0.47** ± 0.02	**0.59** ± 0.03	>0.05	**0.40** ± 0.02[†]	**0.71** ± 0.04[‡]
$_v$BMD (g cm^{-3})	**0.52** ± 0.02	**0.50** ± 0.02	**0.47** ± 0.02	**0.29** ± 0.02	<0.001	--	**0.19** ± 0.01[ΙΙ]
TMD (g cm^{-3})	**1.62** ± 0.01	**1.64** ± 0.01	**1.65** ± 0.01	**1.60** ± 0.01	<0.001	--	--
D^{2D}	**1.72** ± 0.01*	**1.73** ± 0.01	**1.72** ± 0.01	**1.46** ± 0.02	<0.001	--	--
D^{3D}	**2.51** ± 0.02*	**2.54** ± 0.02*	**2.51** ± 0.04	**2.28** ± 0.03	<0.001	--	--
E_z (MPa)	**2408.40** ± 83.62	**2351.52** ± 82.51	**2151.34** ± 98.94	**1164.06** ± 147.40	<0.001	**3230** ± 250[¶]	--

1

3.1 Microarchitecture Characteristics

3   All microarchitectural characteristics for non-fracture males and females have been previously

4   reported by Greenwood, et al (2018) (see Table 1 for reported values). Fracture specimens are

5   made up of a subset of those published previously, and thus results are given here for this

6   subset.

7   Significant differences are present between age-matched non-fracture and fracture females for

8   BV/TV, BS/BV, $_v$BMD and TMD ($p < 0.01$ for all) (Figures 1a-d respectively).

9

3.2 Fractal Dimension

11   No significant age-related trends are observed for non-fracture males and females for both D^{2D}

12   and D^{3D} ($p > 0.05$). However, a significant difference in both D^{2D} and D^{3D} is seen in age-

13   matched populations between non-fracture and fracture females ($p < 0.01$, Figure 1e-f

14   respectively).

15
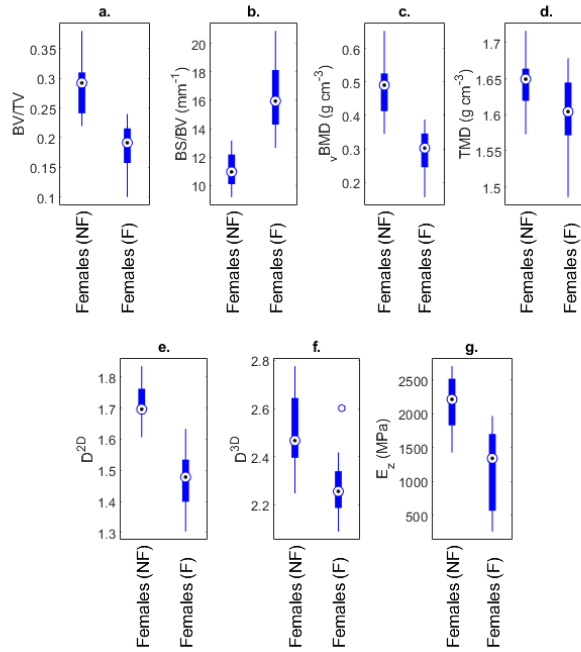
Figure 1: Box and whisker plots for age-matched (73 years +) non-fracture females and fracture females for a) BV/TV, b) BS/BV, c) $_vBMD$, d) TMD, e) D^{2D}, f) D^{3D}, and g) E_z.

3.3 Finite Element Analysis

Apparent modulus was calculated in the z axis (the direction of principle loading within the femur head). E_z is found to have a significant negative trend with age in non-fractured males ($p < 0.05$), but not in non-fracture females ($p > 0.05$). In an age-matched sample, non-fractured females are significantly different from fractured females ($p < 0.01$) as can be seen in Figure 1g.

BV/TV is found to be positively correlated with E_z in non-fracture males and females, and fracture females (Figure 2a). BS/BV is negatively correlated with E_z in non-fracture males and females, as well as fracture females (Figure 2b). D^{2D} is positively correlated with E_z in non-fracture females and fracture females (Figure 2c) but is not correlated in non-fracture males.

D^{3D} is not correlated with E_z in any group. P-values and R^2 values for all linear regressions are given in Table 4.

Table 4: Results of linear regressions for BV/TV vs age, BS/BV vs age, D^{2D} vs age, and D^{3D} vs age, BV/TV vs E$_z$, BS/BV vs E$_z$, D^{2D} vs E$_z$, and D^{3D} vs E$_z$. R^2 values are given for parameters with significant correlations.

	Non-Fracture Males		Non-Fracture Females		Fracture Females		Correlation
Age	**p-value**	**R^2**	**p-value**	**R^2**	**p-value**	**R^2**	
BV/TV	<0.05	0.19	<0.05	0.20	>0.05	--	negative
BS/BV	>0.05	--	>0.05	--	>0.05	--	--
D^{2D}	>0.05	--	>0.05	--	>0.05	--	--
D^{3D}	>0.05	--	>0.05	--	>0.05	--	--
E$_z$	**p-value**	**R^2**	**p-value**	**R^2**	**p-value**	**R^2**	
BV/TV	<0.05	0.56	<0.05	0.51	<0.05	0.53	positive
BS/BV	<0.05	0.51	<0.05	0.48	<0.05	0.33	negative
D^{2D}	>0.05	--	<0.05	0.18	<0.05	0.58	positive
D^{3D}	>0.05	--	>0.05	--	>0.05	--	--
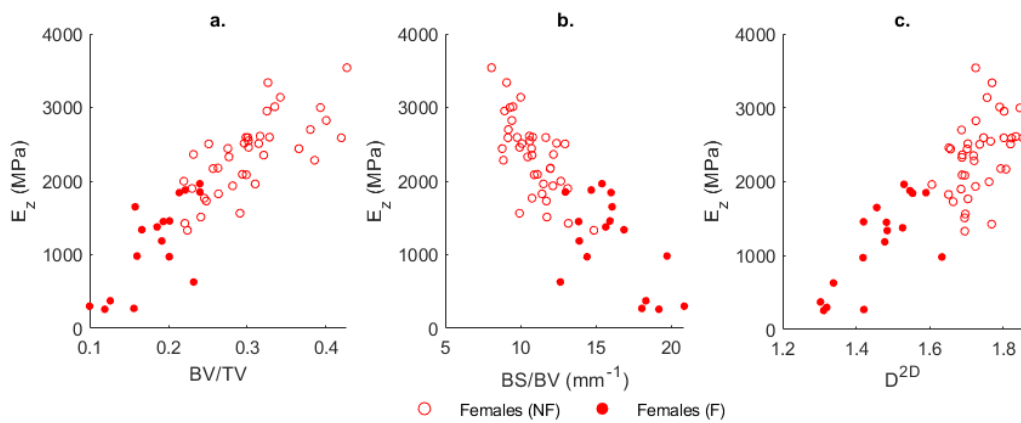
Figure 2: Relationships between a) BV/TV and E$_z$ for non-fracture and fracture females, b) BS/BV and E$_z$ for non-fracture and fracture females, d) D^{2D} and E$_z$ for non-fracture and fracture females.

3.4 Diagnostic Tests

Overall results of diagnostic tests (including sensitivity, specificity and accuracy) are given in Table 5. D^{2D} and BS/BV show the highest sensitivity, specificity, and accuracy.

Table 5: Results of diagnostic tests for several parameters (D^{2D}, D^{3D}, BV/TV, BS/BV, $_vBMD$, TMD and E_z) using the midpoint between the means of age-matched non-fracture females and fracture females as the cut-off point for OP.

Parameter Used	Sensitivity	Specificity	Positive Predictive Value	Negative Predictive Value	Accuracy
D^{2D}	0.88	1.00	1.00	0.10	0.94
D^{3D}	0.82	0.78	0.78	0.18	0.80
BV/TV	0.82	0.78	0.78	0.18	0.80
BS/BV	0.88	1.00	1.00	0.10	0.94
$_vBMD$	0.88	0.89	0.88	0.11	0.89
TMD	0.71	0.65	0.67	0.31	0.68
E_z	0.76	0.83	0.81	0.21	0.80

4 Discussion

Overall, values for microarchitectural characteristics (BV/TV, BS/BV, TbTh, TbSp, $_vBMD$ and TMD), fractal dimension measurements (D^{2D} and D^{3D}) and E_z are consistent with values within literature, both for femoral head studies (Li et al., 2012; Morgan and Keaveny, 2001; Perilli et al., 2008; Wu et al., 2015; Zhang et al., 2010) as well as other bone sites and animal models (Alberich-Bayarri et al., 2010; Jerome et al., 2014; Lill et al 2002; Xie et al., 2018). Differences observed for values of TbTh and TbSp reported in this study and within literature are potentially due to differing assumptions (e.g. sphere, plate) for measurements.

By definition, a high BS/BV corresponds to bone with either very low BV/TV or an unusually high surface area (a very complex surface for the volume present), or both. High BS/BV has been observed previously within induced OP animal models (Jerome et al., 2014; Lill et al., 2002) as well as human samples (Xie et al., 2018), as increased resorption would be initially observed on relatively small features which contribute to greater complexity of trabecular structures.

As TMD affects the tissue's local tissue modulus (Chevalier et al., 2007; van Rietbergen and Ito, 2015) which, for the purposes of this study, was fixed at 10 GPa, TMD did not affect apparent modulus. Further, as $_v$BMD was calculated from BV/TV and TMD, only BV/TV was used within linear regression models with both age and E_z. As there are significant differences in non-fracture and fracture TMD, it is expected that if TMD were to be considered when declaring local tissue modulus, this difference would be reflected within apparent Young's modulus.

D^{2D} and D^{3D} quantitatively characterise the complexity of trabecular structure surfaces relative to the total area (D^{2D}) or total volume (D^{3D}). Past studies have shown that D^{2D} has strong correlation with microarchitectural parameters ($R^2 = 0.50 – 0.85$) (Bauer et al., 2006). Within the present study D^{2D} and D^{3D} are not correlated with age, though both are a good predictor of fracture, which is consistent with previous studies (Alberich-Bayarri et al., 2010; Audran et al, 2001). As D^{2D} and D^{3D} are not normalised to the volume of bone, the increase in R^2 between non-fracture and fracture females (18.04 and 57.67 respectively) may be explained by the reduction in BV/TV within the groups (0.30 and 0.18 respectively) (Chung et al., 1994). With no significant correlations seen for both non-fracture male and female samples for D^{2D} and D^{3D} with age, the differences observed between non-fracture and fracture specimens indicates that osteoporosis may not be just an accelerated aging process, but a disease.

Apparent Young's modulus measured within non-fracture male and female samples is consistent with experimental Young's modulus of samples taken from the femoral head from literature (Chevalier et al., 2007; Morgan and Keaveny, 2001). The predictive power of BMD for Young's Modulus has been well documented both in animal models and in human samples (Alberich-Bayarri et al., 2008; Amin et al., 2011; Chevalier et al., 2007; Ulrich et al., 1999) and is known to explain between 40% - 60% of variance in Young's modulus. Similar relationships have been seen with BV/TV (Nazarian et al., 2007), justifiably as here BV/TV is

1   used to calculate $_v$BMD from quantitative CT data. Similar agreement is seen between BV/TV

2   and E_z within this study with R^2 values between 0.51 and 0.53 for all samples. However, while

3   E_z is significantly different between non-fracture and fracture females, it does not appear to be

4   the best predictor for fracture.

5   A distinction should be made between Young's modulus and compressive strength (whether

6   measured as yield strength or ultimate strength). There is a possibility that if compressive

7   strength were to be included within this study, it may prove to be a better predictor of fracture

8   risk than other parameters used. However, as stated previously, FEA (μ-FEA especially) is

9   computationally expensive and as such it is unlikely for μ-FEA methods to be efficacious for

10   fracture prediction in a clinical setting.

11

12   **5 Conclusion**

13   Though BV/TV and $_v$BMD correlate with age in both non-fracture males and females, and E_z

14   correlates with age in non-fracture males, BS/BV, D^{2D}, D^{3D} and TMD do not correlate with

15   age. These four properties, however, are significantly different between age-matched non-

16   fracture and fracture specimens, indicating OP is a disease, and not just an accelerated aging

17   process. The degradation in trabecular complexity, while potentially only applicable to OP

18   caused by over-resorption, is a more sensitive method than $_v$BMD (and by extension $_a$BMD)

19   for fracture risk prediction within this study. Though currently this method may not be directly

20   applied *in vivo*, there is potential for it to be applied within the peripheral skeleton with the use

21   of HR-pQCT in future studies.

22

23

24

References

Alberich-Bayarri, A., Marti-Bonmati, L., Ṕrez, M.A., Sanz-Requena, R., Lerma-Garrido, J.J., García-Martí, G., Moratal, D., 2010. Assessment of 2D and 3D fractal dimension measurements of trabecular bone from high-spatial resolution magnetic resonance images at 3 T. Med. Phys. 37, 4930–4937. https://doi.org/10.1118/1.3481509

Alberich-Bayarri, A., Marti-Bonmati, L., Sanz-Requena, R., Belloch, E., Moratal, D., 2008. In Vivo Trabecular Bone Morphologic and Mechanical Relationship Using High-Resolution 3-T MRI. Am. J. Roentgenol. 191, 721–726. https://doi.org/10.2214/ajr.07.3528

Amin, S., Kopperdhal, D.L., Melton, L.J., Achenbach, S.J., Therneau, T.M., Riggs, B.L., Keaveny, T.M., Khosla, S., 2011. Association of hip strength estimates by finite-element analysis with fractures in women and men. J. Bone Miner. Res. 26, 1593–1600. https://doi.org/10.1002/jbmr.347

Audran, M., Chappard, D., Legrand, E., Libouban, H., Baslé, M.F., 2001. Bone microarchitecture and bone fragility in men: DXA and histomorphometry in humans and in the orchidectomized rat model. Calcif. Tissue Int. 69, 214–217. https://doi.org/10.1007/s00223-001-1058-2

Bauer, J.S., Kohlmann, S., Eckstein, F., Mueller, D., Lochmüller, E.M., Link, T.M., 2006. Structural analysis of trabecular bone of the proximal femur using multislice computed tomography: a comparison with dual X-ray absorptiometry for predicting biomechanical strength in vitro. Calcif. Tissue Int. 78, 78–89. https://doi.org/10.1007/s00223-005-0070-3

Benhamou, C.L., Poupon, S., Lespessailles, E., Loiseau, S., Jennane, R., Siroux, V., Ohley, W., Pothuaud, L., 2001. Fractal analysis of radiographic trabecular bone texture and bone mineral density: Two complementary parameters related to osteoporotic fractures. J. Bone Miner. Res. 16, 697–704. https://doi.org/10.1359/jbmr.2001.16.4.697

Burghardt, A.J., Link, T.M., Majumdar, S., 2011. High-resolution computed tomography for clinical imaging of bone microarchitecture. Clin. Orthop. Relat. Res. 469, 2179–2193. https://doi.org/10.1007/s11999-010-1766-x

Chevalier, Y., Pahr, D., Allmer, H., Charlebois, M., Zysset, P., 2007. Validation of a voxel-based FE method for prediction of the uniaxial apparent modulus of human trabecular bone using macroscopic mechanical tests and nanoindentation. J. Biomech. 40, 3333–40. https://doi.org/10.1016/j.jbiomech.2007.05.004

Chung, H.W., Chu, C.C., Underweiser, M., Wehrli, F.W., 1994. On the Fractal Nature of Trabecular Structure. Med. Phys. 21, 1535–1540. https://doi.org/10.1118/1.597263

Cody, D.D., Gross, G.J., Hou, F.J., Spencer, H.J., Goldstein, S.A., Fyhrie, D.P., 1999. Femoral strength is better predicted by finite elment models than QCT and DXA. J. Biomech. 32, 1013–1020.

Cortet, B., Boutry, N., Dubois, P., Legroux-Gérot, I., Corten, A., Marchandise, X., 2004. Does Quantitative Ultrasound of Bone Reflect More Bone Mineral Density Than Bone Microarchitecture? Calcif. Tissue Int. 74, 60–67. https://doi.org/10.1007/s00223-002-2113-3

Engelke, K., van Rietbergen, B., Zysset, P., 2016. FEA to Measure Bone Strength: A Review. Clin. Rev. Bone Miner. Metab. 14, 26–37. https://doi.org/10.1007/s12018-015-9201-1

Fazzalari, N.L., Parkinson, I.H., 1996. Fractal dimension and architecture of trabecular bone. J. Pathol. 178, 100–105. https://doi.org/10.1002/(SICI)1096-9896(199601)178:1<100::AID-PATH429>3.0.CO;2-K

Fung, Y.C., 1993. Biomechanics: Mechanical properties of living tissues, 2nd ed, J Springer. https://doi.org/10.1007/978-1-4757-2257-4

Greenwood, C., Clement, J., Dicken, A., Evans, P., Lyburn, I., Martin, R.M., Stone, N., Zioupos, P., Rogers, K., 2018. Age-Related Changes in Femoral Head Trabecular Microarchitecture. Aging Dis. 9, 976. https://doi.org/10.14336/ad.2018.0124

International Osteoporosis Foundation, 2015. Broken Bones, Broken Lives: A Roadmap to Solve the Fragility Fracture Crisis in the United Kingdom. Nyon.

Jerome, C.P., Vafai, H.T., Minetti, K.L., Kaplan, K., 2014. Structural Histomorphometric Analysis of Cortical, Transitional, and Cancellous Vertebral Bone in Intact, Ovariectomized, and Nandrolone-Treated Cynomolgus Monkeys (Macaca fascicularis). J. Histotechnol. 20, 191–198. https://doi.org/10.1179/his.1997.20.3.191

Jiang, C., Giger, M.L., Chinander, M.R., Martell, J.M., Kwak, S., Favus, M.J., 1999. Characterization of bone quality using computer-extracted radiographic features. Med. Phys. 26, 872–879. https://doi.org/10.1118/1.598604

Kanis, J.A., McCloskey, E. V, Johansson, H., Cooper, C., Rizzoli, R., Reginster, J.Y., 2013. European guidance for the diagnosis and management of osteoporosis in postmenopausal women. Osteoporos. Int. 24, 23–57. https://doi.org/10.1007/s00198-012-2074-y

Keaveny, T.M., Kopperdahl, D.L., Melton, L.J., Hoffmann, P.F., Amin, S., Riggs, B.L., Khosla, S., 2010. Age-dependence of femoral strength in white women and men. J. Bone Miner. Res. 25, 994–1001. https://doi.org/10.1002/jbmr.091033

Kopperdahl, D.L., Aspelund, T., Hoffmann, P.F., Sigurdsson, S., Siggeirsdottir, K., Harris, T.B., Gudnason, V., Keaveny, T.M., 2014. Assessment of incident spine and hip fractures in women and men using finite element analysis of CT scans. J. Bone Miner. Res. 29, 570–580. https://doi.org/10.1002/jbmr.2069

Li, Z.C., Dai, L.Y., Jiang, S., Qiu, S., 2012. Difference in subchondral cancellous bone between postmenopausal women with hip osteoarthritis and osteoporotic fracture: Implication for fatigue microdamage, bone microarchitecture, and biomechanical properties. Arthritis Rheum. 64, 3955–3962. https://doi.org/10.1002/art.34670

Lill, C.A., Fluegel, A.K., Schneider, E., 2002. Effect of ovariectomy, malnutrition and glucocorticoid application on bone properties in sheep: A pilot study. Osteoporos. Int. 13, 480–486. https://doi.org/10.1007/s001980200058

MacNeil, J.A., Boyd, S.K., 2008. Bone strength at the distal radius can be estimated from high-resolution peripheral quantitative computed tomography and the finite element method. Bone 42, 1203–1213. https://doi.org/10.1016/j.bone.2008.01.017

Morgan, E.F., Keaveny, T.M., 2001. Dependence of yield strain of human trabecular bone on anatomic site. J. Biomech. 34, 569–577. https://doi.org/10.1016/S0021-9290(01)00011-2

Naylor, K.E., McCloskey, E. V, Eastell, R., Yang, L., 2013. Use of DXA-based finite element analysis of the proximal femur in a longitudinal study of hip fracture. J. Bone Miner. Res. 28, 1014–1021. https://doi.org/10.1002/jbmr.1856

1 Nazarian, A., Muller, J., Zurakowski, D., Müller, R., Snyder, B.D., 2007. Densitometric,
2   morphometric and mechanical distributions in the human proximal femur. J.
3   Biomech. 40, 2573–2579. https://doi.org/10.1016/j.jbiomech.2006.11.022

4 Newitt, D.C., Majumdar, S., van Rietbergen, B., von Ingersleben, G., Harris, S.T., Genant,
5   H.K., Chesnut, C., Garnero, P., MacDonald, B., 2002. In Vivo Assessment of
6   Architecture and Micro-Finite Element Analysis Derived Indices of Mechanical
7   Properties of Trabecular Bone in the Radius. Osteoporos. Int. 13, 6–17.
8   https://doi.org/10.1007/s198-002-8332-0

9 NHS, 2016. Osteoporosis [WWW Document]. URL
10   https://www.nhs.uk/conditions/osteoporosis/ (accessed 6.18.19).

11 Osterhoff, G., Morgan, E.F., Shefelbine, S.J., Karim, L., McNamara, L.M., Augat, P., 2016.
12   Bone mechanical properties and changes with osteoporosis. Injury 47, S11–S20.
13   https://doi.org/10.4172/2157-7633.1000305.Improved

14 Perilli, E., Baleani, M., Öhman, C., Fognani, R., Baruffaldi, F., Viceconti, M., 2008.
15   Dependence of mechanical compressive strength on local variations in
16   microarchitecture in cancellous bone of proximal human femur. J. Biomech. 41, 438–
17   446. https://doi.org/10.1016/j.jbiomech.2007.08.003

18 Teo, J.C.M., Si-Hoe, K.M., Keh, J.E.L. and Teoh, S.H. (2006) 'Relationship between CT
19   intensity, micro-architecture and mechanical properties of porcine vertebral
20   cancellous bone', Clinical Biomechanics, 21(3), pp. 235–244.

21 Ulrich, D., Van Rietbergen, B., Laib, A., Ṙuegsegger, P., 1999. The ability of three-
22   dimensional structural indices to reflect mechanical aspects of trabecular bone. Bone
23   25, 55–60. https://doi.org/10.1016/S8756-3282(99)00098-8

24 van Rietbergen, B., Ito, K., 2015. A survey of micro-finite element analysis for clinical
25   assessment of bone strength: The first decade. J. Biomech. 48, 832–841.
26   https://doi.org/10.1016/j.jbiomech.2014.12.024

27 Wu, D., Li, X., Tao, C., Dai, R., Ni, J., Liao, E., 2015. Association of microstructural and
28   mechanical properties of cancellous bone and their fracture risk assessment tool
29   scores. Int. J. Clin. Exp. Med. 8, 3956–3964.

Xie, F., Zhou, B., Wang, J., Liu, T., Wu, X., Fang, R., Kang, Y., Dai, R., 2018. Microstructural properties of trabecular bone autografts: comparison of men and women with and without osteoporosis. Arch. Osteoporos. 13. https://doi.org/10.1007/s11657-018-0422-z

Yerramshetty, J.S. and Akkus, O. (2013) 'Changes in Cortical Bone Mineral and Microstructure with Aging and Osteoporosis', in Silva, M. J. (ed.) Skeletal Aging and Osteoporosis. , pp. 105–131.

Zhang, Z.M., Li, Z.C., Jiang, L.S., Jiang, S.D., Dai, L.Y., 2010. Micro-CT and mechanical evaluation of subchondral trabecular bone structure between postmenopausal women with osteoarthritis and osteoporosis. Osteoporos. Int. 21, 1383–1390. https://doi.org/10.1007/s00198-009-1071-2

Declaration of interests

☒ The authors declare that they have no known competing financial interests or personal relationships that could have appeared to influence the work reported in this paper.

☐The authors declare the following financial interests/personal relationships which may be considered as potential competing interests:

1 Study design: JC, KDR, CG. Study conduct: JC, KDR, CG. Data collection: CG, JC, FGC.

2 Data analysis: CG, ELA. Data interpretation: ELA, CG, KDR. Drafting manuscript: ELA.

3 Revising manuscript content: CG, KDR. Approving final version of manuscript: ELA, CG,

4 KDR, FGC. EA takes responsibility for the integrity of the data analysis.